Available online at www.sciencedirect.com
SCIENCE DIRECT®
International Journal of Mass Spectrometry 225 (2003) 167–176
International Journal of Mass Spectrometry
www.elsevier.com/locate/ijms

Hybrid DFT study on the gas-phase S_N2 reactions at neutral oxygen

Yi Ren [a,*], Joel L. Wolk [b], Shmaryahu Hoz [b]

[a] *Faculty of Chemistry, Sichuan University, Chengdu 610064, PR China*
[b] *Department of Chemistry, Bar-Ilan University, Ramat-Gan 52900, Israel*

Received 5 October 2002; accepted 28 November 2002

Abstract

The hybrid DFT method MPW1K, in conjunction with 6-31+G(d,p) basis sets, has been examined for the gas-phase reactions, $Y^- + HOX$ (Y, X = F, Cl, Br, I). Comparison of the results with the high-level G2(+) theory indicates that MPW1K/6-31+G(d,p) approach performs well in describing the potential energy surface for the identity S_N2 reactions $X^- + HOX \rightarrow HOX + X^-$ (X = Cl, Br, I). The corresponding non-identity reactions (Y ≠ X, Y, X = Cl, Br, I), are exothermic if the nucleophile is the heavier halide, in contrast to the corresponding reactions at carbon. The fluorine behaves different from the other halogens. The reactions $Y^- + HOF$ (Y = F, Cl, Br, I) are predicted to form the energetically favorable products $YO^- + HF$ with a large driving force($\Delta H = -48.6, -47.2, -56.5, -69.0$ kJ/mol for Y = F, Cl, Br, I, respectively) and lower reaction enthalpies than the corresponding S_N2 reactions by about 60 kJ/mol. Central barrier heights ($\Delta H^{\neq}_{YX}$) for S_N2 reactions in the exothermic directions vary from 52.5 kJ/mol for Y = I, X = Br up to 76.6 kJ/mol for Y = Br, X = Cl. Overall barriers (ΔH^{b}_{YX}) for reactions in the exothermic direction are all negative (varying from −13.8 kJ/mol for Y = I, X = Br to −5.2 kJ/mol for Y = Br, X = Cl). Complexation energies (ΔH^{comp}) of the ion–molecule complexes $Y^- \cdots HOX$ vary from 66.3 kJ/mol for Y = I, X = Br to 95.5 kJ/mol for Y = Cl, X = Br. The central barrier heights $\Delta H^{\neq}_{YX}$ and $\Delta H^{\neq}_{XY}$ correlate well with the degree of the O–X and O–Y bond elongation in the transition structures. Both central and overall barriers can be interpreted with the aid of Marcus equation.

Keywords: S_N2 at neutral oxygen; Hybrid DFT method; Reaction mechanism

1. Introduction

Bimolecular nucleophilic substitutions (S_N2) at carbon are among the most intensively studied of all chemical reactions. Recently, the mechanisms of the S_N2 reactions at heteroatoms have become the focus of increasing attention, both experimental [1–5] and theoretical [6–10], because of their synthetic, biochemical, chemical, and theoretical importance. Theoretical studies have revealed similarities and differences between nucleophilic substitution at heteroatoms and at carbon [8–10]. We recently examined the gas-phase identity nucleophilic substitution at neutral oxygen [10]. At the G2(+) level of theory, the reactions $X^- + HOX \rightarrow HOX + X^-$ (X = F, Cl, Br, I) follow an S_N2 pathway with a single transition state connecting the reactant and product ion–molecule complexes.

* Corresponding author.
E-mail address: yiren57@sc.homeway.com.cn (Y. Ren).

1387-3806/02/$ – see front matter
PII S1387-3806(02)01113-2

Our studies also led to the important conclusions: (1) the central barrier heights for the reaction $X^- + HOX$ (X = F, Cl, Br, I) lie within a significantly larger range, about 48 kJ/mol, than those for the corresponding nucleophilic substitutions at carbon and nitrogen; (2) the overall barriers are negative for all halogens; and (3) the fluorine behaves in many respects different than the other halogens. This phenomenon may be attributed a slighter stronger acidity of HOF than HF in gas phase. The deprotonation reaction $F^- + HOF \rightarrow HF + OF$ (exothermic) instead of displacement reaction $F^- + HOF \rightarrow HOF + F^-$ (endothermic) is perhaps the best "candidate" for observation in the gas phase.

Hybrid Hartree–Fock density–function theory (hereafter called hybrid DFT) is of great interest for computational thermochemistry and thermochemical kinetics. Its low computational cost compared to high-level ab initio methods makes it a very attractive alternative for many applications. Recently, Truhlar and coworkers proposed a new hybrid DFT model called the modified Perdew–Wang 1-parameter-method for kinetics (MPW1K) [11]. They checked 20 test reactions and found that the MPW1K/6-31+G(d,p) level reduced the mean unsigned error (MUE) in reaction barrier heights by a factor of 2.4 over MPW1PW and by a factor of 3 over B3LYP. Parthiban and coworkers [12] studied the gas-phase S_N2 reactions at carbon $Y^- + CH_3X \rightarrow CH_3Y + X^-$ (X, Y = F, Cl, Br) using a series of high-level ab initio computational thermochemistry methods and eight density functional methods and concluded that the MPW1K functional performs of all the DFT methods tested.

In our previous paper [13], the gas-phase identity S_N2 reactions at neutral nitrogen $X^- + NH_2X \rightarrow NH_2X + X^-$ (where X = F, Cl, Br, I) were studied using the three hybrid DFT methods B3LYP, MPW1PW, and MPW1K. The results confirm the success for energies and geometries of the MPW1K method with 6-31+G(d,p) basis sets in studying the identity S_N2 reactions at neutral nitrogen.

In this paper, we report our application of the MPW1K method to the nucleophilic substitution reactions at neutral oxygen:

$$Y^- + HOX \rightarrow YOH + X^- \quad (Y, X = F, Cl, Br, I) \tag{1}$$

It should be emphasized that experimental data for these S_N2 reactions are not available. Therefore, it would be appropriate to compare the performance of the hybrid MPW1K method with that of the higher level G2(+) theory. One of the goals of this work is to check how accurately the hybrid DFT method can predict the geometrical structures and potential energy surfaces involved in the identity S_N2 reactions at oxygen. We also wish to test the applicability of Marcus theory [14–16] and the additivity postulate [15] for central barrier heights as applied to gas-phase S_N2 reactions at carbon and nitrogen.

2. Methods

All structures of reactants, ion–molecule complexes, transition states, and products were completely optimized at the MPW1K level with the 6-31+G(d,p) basis sets [11] using GAUSSIAN 98 [17]. All electron (AE) calculations were run for the fluorine- and chlorine-containing species, while Wadt and Hay [18] effective core potentials (MPW1K-ECP) were used for bromine- and iodine-containing species.

Stationary points on potential energy surfaces were characterized using analytical frequencies: all ground states had only real frequencies and all transition states had one and only one imaginary frequency. A scaling factor of 0.9515 [19] was used for zero-point vibrational energy (ZPVE) corrections in the calculation of relative energies for the various species involved in Eq. (1).

Throughout this paper, bond lengths are in angstroms (Å), and bond angles are in degrees (°). Relative energies correspond to enthalpy changes at 0 K [ΔH (0 K)].

3. Results and discussion

The gas-phase reaction profile for the concerted S_N2 reaction at oxygen is described by a symmetrical

double-well potential curve for the identity reactions or an asymmetric double-well potential curve for the non-identity reactions. The reaction involves the initial formation of a reactant ion–molecule complex **1**. This complex must then overcome the central activation barrier to reach a symmetrical or asymmetrical transition structure **2**. The latter then breaks down to give the product ion–molecule complex **3** which subsequently dissociates into the separate products. Analysis of the overall enthalpy changes indicates that the gas-phase non-identity S_N2 reaction at oxygen is endothermic if the nucleophile is the lighter halide, in contrast to the non-identity S_N2 reactions at carbon [20]. In the following discussion, the forward reactions are defined as those which are exothermic.

The key energetic quantities involved in reactions (Eq. (1)), as depicted in Fig. 1, are labeled as follows: ΔH_{YX}^{comp} and ΔH_{XY}^{comp} are the complexation energies for the ion–molecule complexes **1** and **3**, respectively. $\Delta H_{YX}^{\neq}$ and $\Delta H_{XY}^{\neq}$ are the central activation barriers, and ΔH_{YX}^{b} and ΔH_{XY}^{b} are the overall activation barriers, for the corresponding forward and reverse reactions. ΔH is the central enthalpy difference between the product and reactant ion–molecule complexes **1** and **3**. ΔH^{ovr} is the overall enthalpy change for the forward reaction.

$$\Delta H_{YX}^{comp} = H(HOX) - H(Y^-) - H(Y^- \cdots HOX) \quad (2)$$

$$\Delta H_{XY}^{comp} = H(HOY) - H(X^-) - H(YOH \cdots X^-) \quad (3)$$

$$\Delta H_{YX}^{\neq} = H[(Y \cdots HO \cdots X)^{-\neq}] - H(Y^- \cdots HOX) \quad (4)$$

$$\Delta H_{XY}^{\neq} = H[(Y \cdots HO \cdots X)^{-\neq}] - H(YOH \cdots X^-) \quad (5)$$

$$\Delta H_{YX}^{b} = H[(Y \cdots HO \cdots X)^{-\neq}] - H(HOX) - H(Y^-) \quad (6)$$

$$\Delta H_{XY}^{b} = H[(Y \cdots HO \cdots X)^{-\neq}] - H(HOY) - H(X^-) \quad (7)$$

$$\Delta H = H(YOH \cdots X^-) - H(Y^- \cdots HOX) \quad (8)$$

$$\Delta H^{ovr} = H(HOY) + H(X^-) - H(HOX) - H(Y^-) \quad (9)$$

3.1. Hypohalous acids HOX structures (X = F, Cl, Br, I)

Geometries of HOX calculated at the MPW1K/6-31+G(d,p) level are presented in Table 1. The bond lengths in the HOX geometries at the MPW1K/6-31+G(d,p) level generally agree well with the experimental data [21] except the O–F bond length in HOF,

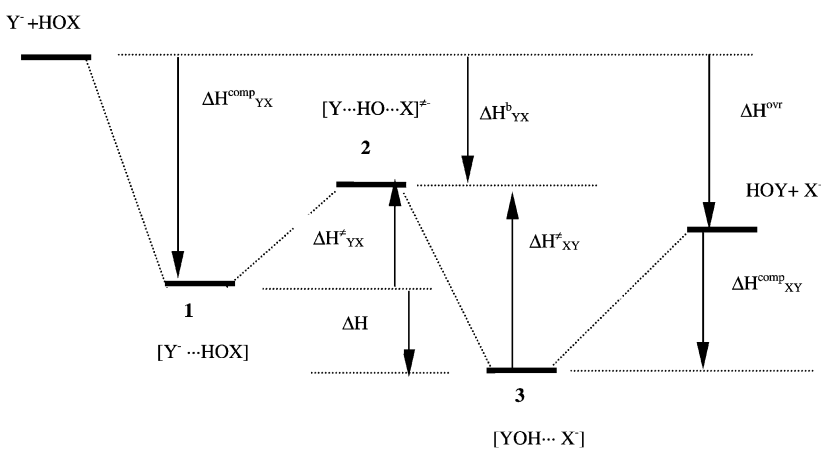

Fig. 1. Schematic potential energy surface for the gas-phase displacement reaction $Y^- + HOX \rightarrow YOH + X^-$ (Y, X = Cl, Br, I).

Table 1
Calculated geometries of HOX (X = F, Cl, Br, I)

	Computational level	r(H–O)	r(O–X)	∠H–O–X
X = F	MPW1K/6-31+G(d,p)	0.962	1.396	99.3
	MP2/6-31+G(d)[a]	0.981	1.454	97.3
	Experimental[b]	0.966	1.442	96.8
X = Cl	MPW1K/6-31+G(d,p)	0.959	1.679	104.4
	MP2/6-31+G(d)[a]	0.980	1.718	103.5
	Experimental[b]	0.964	1.689	103.0
X = Br	MPW1K/6-31+G(d,p)	0.959	1.823	104.8
	MP2/6-31+G(d)[a]	0.981	1.869	103.3
	Experimental[b]	0.961	1.834	102.3
X = I	MPW1K/6-31+G(d,p)	0.958	1.977	106.8
	MP2/6-31+G(d)[a]	0.981	2.019	105.3
	Experimental[b]	0.960	1.959–1.995	102.4

[a] From [10].
[b] From [21].

which is significantly underestimated. All of the angles ∠H–O–X are slightly overestimated and the calculated ∠H–O–X differ from experimental values by up to 4.4°. Comparing with the experimental data, the mean signed errors (MSEs) for the bond lengths in the HOX are only −0.01 Å at the MPW1K/6-31+G(d,p) level and 0.02 Å at the MP2/6-31+G(d) level [10], respectively.

3.2. Ion–molecule complexes

Two conformers are known for the ion–molecule complexes. Previous studies suggested that complexes in which the halide ion coordinates with the HOX through the hydrogen are lower in energy than those in which the halide anion complexes with the halogen to form a so-called "X-philic" pre-reaction complex ($HOX\cdots Y^-$). For the $Cl^-\cdots HOBr$ and $Br^-\cdots HOCl$ species, Flowers and Francisco [22] found that the minimum energy structure involves complexation with the hydrogen of the hypohalous acid. At the CCSD(T)/6-311++G(2df,2p)+ΔZPVE level, the total energy of $Cl^-\cdots HOBr$ is lower than $Cl^-\cdots BrOH$ by 10.9 kJ/mol, while $Br^-\cdots HOCl$ is lower in energy than $Br^-\cdots ClOH$ by 42.2 kJ/mol. Therefore, X-philic complexes are not considered here.

3.2.1. Geometries

The geometries of the complexes are listed in Table 2. Comparison of the MPW1K/6-31+G(d,p) geometries of $X^-\cdots HOX$ (X = F, Cl, Br, I) with the G2(+) structural data shows reasonable agreement except for the O–H and F–H bonds in $F^-\cdots HOF$. The MPW1K/6-31+G(d,p) method predicts too short $F\cdots H$ distance and too high interaction energy, which will induce the overestimation of the complexation energy for the F^- + HOF system. The MSEs and the MUEs for the bond lengths in $X^-\cdots HOX$ (X = F–I) are −0.03 and 0.04 Å, respectively.

We were unable to locate the stable complexes $YOH\cdots F^-$ (Y = Cl, Br, I) that corresponded to **3** in Fig. 1. The "oxygen transfer" reactions $Y^- + HOF \rightarrow HF + OY^-$ (Y = Cl, Br, I) instead of displacement reactions $Y^- + HOF \rightarrow HOY + F^-$ will be favorable when Y^- interacts with HOF (Y = Cl, Br, I), respectively, which are expected because of the much stronger acidity of HOX (Cl, Br, I) than HF.

For the geometries of complexes $Y^-\cdots HOX$ (Y ≠ X, Y, X = Cl, Br, I), the MPW1K/6-31+G(d,p) geometries are also close to the results of higher level. For example, our calculated geometries of $Cl^-\cdots HOBr$ and $Br^-\cdots HOI$ are almost equal to the parameters reported by Flowers and Francisco at the CCSD(T)/6-311++G(2df,2p) level [22].

Table 2
Geometries for all of the ion–molecule complexes at the MPW1K/6-31+G(d,p) level in the reactions $Y^- + HOX$ and relative elongation of the O–H bond (%O–H)

	r(Y–H)	r(H–O)	r(O–X)	∠H–O–X	%O–H
$F^- \cdots HOF$	1.104	1.230	1.438	102.4	27.9
[10][a]	1.212	1.173	1.474	101.0	19.6
$Cl^- \cdots HOF$	1.926	1.012	1.410	101.1	5.2
$Br^- \cdots HOF$	2.158	1.000	1.408	100.9	4.0
$I^- \cdots HOF$	2.417	0.992	1.406	100.8	3.1
$Cl^- \cdots HOCl$	1.910	1.014	1.675	105.5	5.7
[10][a]	1.961	1.026	1.708	104.6	4.7
$Br^- \cdots HOCl$	2.137	1.001	1.675	105.4	4.4
[22][b]	2.130	1.004	1.699	103.5	
$I^- \cdots HOCl$	2.405	0.992	1.676	105.2	3.4
$Cl^- \cdots HOBr$	1.907	1.014	1.811	105.9	5.7
[22][b]	1.912	1.016	1.824	103.9	
$Br^- \cdots HOBr$	2.136	1.001	1.812	105.6	4.4
[10][a]	2.180	1.028	1.854	104.3	
$I^- \cdots HOBr$	2.395	0.992	1.815	105.4	3.4
$Cl^- \cdots HOI$	1.918	1.011	1.955	106.9	5.5
$Br^- \cdots HOI$	2.145	0.998	1.957	106.6	4.2
$I^- \cdots HOI$	2.403	0.989	1.961	106.5	3.2
[10][a]	2.421	1.011	2.001	105.3	3.1

[a] Geometries were optimized at the MP2/6-31+G(d) level.
[b] Geometries were optimized at the CCSD(T)/6-311++G(2df,2p) level.

The geometries of the HOX moieties in the $Y^- \cdots HOX$ or $X^- \cdots HOY$ species differ from those of the unperturbed reactants HOX (or HOY). Thus, the ion–molecule complexes **1** and **3** are characterized by a slight elongation of the H–O and O–X (O–Y) bonds and an increase in angle ∠H–O–X (or ∠H–O–Y) relative to the values in the isolated molecules HOX (HOY). The extent of elongation of the O–H bond can be denoted by the parameter %O–H defined by the Eq. (10), where r^{comp}(O–H) and r^{react}(O–H) are the O–H bond lengths in the ion–molecule complex **1** or **3** and in the reactant HOX molecule, respectively:

$$\%O\text{–}H = \frac{100[r^{comp}(O\text{–}H) - r^{react}(O\text{–}H)]}{r^{react}(O\text{–}H)} \quad (10)$$

There is a well-defined linear relationship between %O–H and the complexation energies ($R^2 = 0.957$).

3.2.2. Complexation energies

The series of the MPW1K/6-31+G(d,p) complexation energies are given in Table 4. First of all, we note that the complexation energies for identity reactions $X^- \cdots HOX$ (X = Cl, Br, I) are very close to the G2(+) results and the largest error is only 1.7 kJ/mol. As for the reaction $F^- + HOF$, the hybrid DFT method significantly overestimate the ΔH^{comp} values by about 20 kJ/mol, which is the similar to our previous studies on the S_N2 at nitrogen using hybrid DFT methods.

The data in Table 4 also show that the complexation enthalpies for $Y^- \cdots HOX$ depend primarily on the identity of nucleophile, and only to a small extent on the identity of HOX, and tend to decrease in their order of basicity in gas phase: $F^- > Cl^- > Br^- > I^-$, that is analogous to the trend found for $Y^- \cdots CH_3X$ [20]. Thus, the complexation energies for $F^- \cdots HOF$ is 207.0 kJ/mol, those for Y = Cl^- range between 92.1 and 100.0 kJ/mol, those for Br^- range between

Table 3
Calculated geometries of the $[Y\cdots HO\cdots X]^{-\neq}$ transition states and the relative elongation of the O–X and O–Y bond

$[Y\cdots HO\cdots X]^{-\neq}$	$r(Y\cdots O)$	$r(O\cdots X)$	r(O–H)	∠Y–O–H	∠H–O–X	%O–$X^{\neq}$	%O–$Y^{\neq}$
$[F\cdots HO\cdots F]^{-\neq}$	1.755, **1.766**[a]		0.952, **0.968**	83.2, **84.4**		22.0, **19.8**	
$[Cl\cdots HO\cdots Cl]^{-\neq}$	2.115, **2.109**		0.959, **0.979**	87.3, **89.4**		26.3, **23.5**	
$[Br\cdots HO\cdots Br]^{-\neq}$	2.231, **2.237**		0.960, **0.984**	88.7, **91.0**		23.1, **20.7**	
$[I\cdots HO\cdots I]^{-\neq}$	2.371, **2.381**		0.962, **0.989**	90.9, **94.4**		20.9, **19.0**	
$[Cl\cdots HO\cdots F]^{-\neq}$	2.107	1.772	0.956	88.4	81.4	25.7	
$[Br\cdots HO\cdots F]^{-\neq}$	2.267	1.739	0.957	87.0	84.4	23.5	
$[I\cdots HO\cdots F]^{-\neq}$	2.471	1.701	0.958	86.1	87.3	21.0	
$[Br\cdots HO\cdots Cl]^{-\neq}$	2.274	2.076	0.960	86.1	89.8	23.9	25.6
$[I\cdots HO\cdots Cl]^{-\neq}$	2.479	2.024	0.961	84.9	92.7	20.7	26.8
$[I\cdots HO\cdots Br]^{-\neq}$	2.445	2.165	0.962	87.0	92.5	24.9	19.3

[a] The geometries at the MP2/6-31+G(d) level [10] are given in bold.

77.6 and 84.5 kJ/mol, while those for I^- range between 64.2 and 70.3 kJ/mol.

For a given HOX, the complexation energies show a good linear correlation with the electronegativities of the halogen Y^- ($R^2 \approx 0.993$ for X = Cl, Br, I, respectively), which is similar to the results for the complexes $Y^-\cdots CH_3X$ [20].

3.3. Transition state structures and barrier heights

MPW1K/6-31+G(d,p) geometries of the transition state structures $[Y\cdots HO\cdots X]^{-\neq}$ are presented in Table 3. The central barriers and overall barriers are included in Table 4.

3.3.1. Geometries

The transition state structures at the MPW1K/6-31+G(d,p) level of theory are found to have C_{2v} symmetry for $[X\cdots HO\cdots X]^{-\neq}$ or C_s symmetry for $[Y\cdots HO\cdots X]^{-\neq}$ (Y ≠ X). The key transition state parameter for appraising the behavior of the hybrid DFT method is the distance between the halogen anion and the oxygen atom. For the identity reactions, the O···X bond lengths in $[X\cdots HO\cdots X]^{-\neq}$ (X = F, Cl, Br, I) calculated by the MPW1K model reproduce very well the G2(+) results. Almost all of the bond lengths in $[X\cdots HO\cdots X]^{-\neq}$ are slightly underestimated at the MPW1K /6-31+G(d,p) level, the MUE and MSE being 0.014 and −0.014 Å, respectively.

Table 4
Energetics (kJ/mol) of the $Y^- + HOX \rightarrow HOY + X^-$ reactions

Y, X	ΔH_{YX}^{comp}	$\Delta H_{YX}^{\neq}$	ΔH_{YX}^{b}	ΔH_{XY}^{b}	$\Delta H_{XY}^{\neq}$	ΔH_{XY}^{comp}	ΔH	ΔH^{ovr}
F, F	207.0 (187.9)[a]	139.5 (106.3)	−67.5 (−81.7)					
Cl, Cl	97.3 (97.5)	94.4 (92.5)	−2.9 (−5.1)					
Br, Br	80.0 (81.2)	71.7 (70.3)	−8.3 (−10.7)					
I, I	64.2 (66.5)	55.5 (58.6)	−8.7 (−8.1)					
Cl, F	100.0	75.8	−24.2					*13.0*[b], ***−47.2***[c]
Br, F	84.5	62.0	−22.6					*11.6*, ***−56.5***
I, F	70.3	49.3	−21.0					*−2.7*, ***−69.0***
Br, Cl	81.7	76.6, **75.6**[d]	−5.2, **−6.3**	−3.8, **−4.9**	91.7, **90.8**	95.5	−15.2	−1.4
I, Cl	67.7	59.7, **56.3**	−8.1, **−13.4**	7.6, **2.2**	99.7, **96.3**	92.1	−40.0	−15.6
I, Br	66.3	52.5, **51.6**	−13.8, **−15.4**	0.4, **−1.2**	77.6, **76.8**	77.2	−25.1	−14.3

[a] Values in parentheses are corresponding energetics at the G2(+) level for the reactions $X^- + HOX$.
[b] Values in italic are reaction enthalpies of supposed S_N2 reactions $Y^- + HOF \rightarrow HOY + F^-$ at the level of MPW1K/6-31+G(d,p).
[c] Values in italic bold are reaction enthalpies of reactions $Y^- + HOF \rightarrow OY^- + HF$ at the level of MPW1K/6-31+G(d,p).
[d] Values in bold are the calculated central barriers with Eq. (14) and overall barriers with Eq. (15).

The main geometric feature in the transition structure is the elongation of the O–X and O–Y bonds relative to the ion–molecular complex. We can readily define the geometrical looseness in the transition structures, %O–X$^{\neq}$ and %O–Y$^{\neq}$, in a manner similar to our previous paper [10].

$$\%\text{O–X}^{\neq} = 100\frac{r^{\neq}(\text{O–X}) - r^{\text{comp}}(\text{O–X})}{r^{\text{comp}}(\text{O–X})} \quad (11)$$

$$\%\text{O–Y}^{\neq} = 100\frac{r^{\neq}(\text{O–Y}) - r^{\text{comp}}(\text{O–Y})}{r^{\text{comp}}(\text{O–Y})} \quad (12)$$

where $r^{\neq}$ and r^{comp} are the bond lengths in the transition structure **2** and ion–molecular complex (**1** or **3**), respectively. As can be seen from the plot in Fig. 2, there is a linear relationship between the central barrier heights and the looseness of the transition structure ($R^2 = 0.957$).

3.3.2. Barriers

The MPW1K functional also predicts central barrier heights and overall barrier heights for the $X^- \cdots HOX$ (X = Cl, Br, I) systems close to the G2(+) results, but significantly overestimates the central barriers for the $F^- \cdots HOX$. The MUEs for the identity reactions (X = Cl, Br, I) are 2.13 kJ/mol (central barriers) and 1.73 kJ/mol (overall barriers). As for the non-identity reactions, the central barriers calculated at 0 K range from 52.5 kJ/mol for the forward reaction $I^- + HOBr$ up to 99.7 kJ/mol for the reverse reaction $Cl^- + HOI$. The forward central barrier heights $\Delta H^{\neq}_{YX}$ are lower than the intrinsic central barrier $\Delta H^{\neq}_{0\,YX}$, while the reverse central barrier heights $\Delta H^{\neq}_{XY}$ are higher than $\Delta H^{\neq}_{0\,YX}$. These results are all expected since the identity reactions are thermoneutral, while the non-identity forward reactions are all expressed as exothermic directions. According to the Marcus theory [14,15], in an exothermic reaction, a thermodynamic driving force will lower the transition state energy, whereas endothermic reactions will induce a higher activation energy. $\Delta H^{\neq}_{0\,YX}$ is estimated using the additivity postulate [15]:

$$\Delta H^{\neq}_{0\,YX} = 0.5[\Delta H^{\neq}_{YY} + \Delta H^{\neq}_{XX}] \quad (13)$$

in which $\Delta H^{\neq}_{YY}$ and $\Delta H^{\neq}_{XX}$ are the central barriers for the identity S_N2 reactions.

The forward overall barriers ΔH^{b}_{YX} for $Y^- + HOX$ are all negative, analogous to the corresponding values for identity substitution reaction at oxygen, but in the reverse direction only the overall barrier for the reaction $Cl^- + HOBr$ is negative.

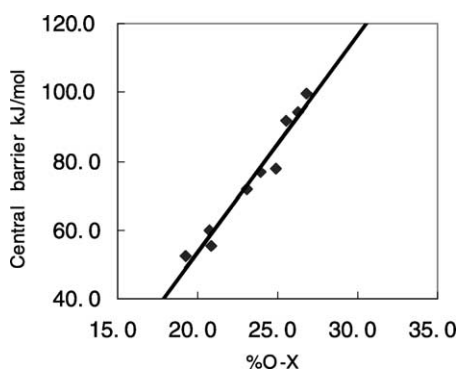

Fig. 2. Plot of MPW1K/6-31+G(d,p) central barriers for S_N2 reactions $Y^- + HOX \rightarrow HOY + X^-$ (Y, X = Cl, Br, I) vs. the geometric looseness index of transition structures **2** (see Eqs. (11) and (12)). The values are presented in Table 3.

3.4. Proton transfer (PT)

PT reactions are important processes that can compete potentially with S_N2 displacement. Our studies show that only $F^- + HOX \rightarrow HF + OX^-$ (X = F, Cl, Br, I) is exothermic and the other PT reactions $Y^- + HOX \rightarrow HY + OX^-$ (Y = Cl, Br, I; X = F, Cl, Br, I) are endothermic, which means that the PT reactions $F^- + HOX$ (Y = F, Cl, Br, I) are energetically favorable and the reactions $Y^- + HOF$ (X = F, Cl, Br, I) will lead to "oxygen transfer" products $OY^- + HF$. The calculated PT reaction enthalpies differ from experimental data [23] by up to about 26 kJ/mol. Table 5 displays all of the possible enthalpies of PT reactions along with the corresponding experimental values at 298 K.

3.5. Rate–equilibrium relationship

Marcus theory has been successfully applied to the interpretation of gas-phase S_N2 reactions at carbon

Table 5
Overall enthalpy changes (kJ/mol) in the deprotonation reactions $Y^- + HOX \rightarrow HY + OX^-$ (kJ/mol) at the MPW1K/6-31+G(d,p) level at 0 K and the corresponding experimental data [23] in parentheses at 298 K

HOX	$Y = F^-$	$Y = Cl^-$	$Y = Br^-$	$Y = I^-$
HOF	−48.6 (−37.8 ± 13)	127.6 (122.0 ± 14)	172.5 (163.5 ± 14)	209.6 (202.0 ± 14)
HOCl	−60.2 (−66.8 ± 4)	116.1 (93.0 ± 5)	161.0 (134.5 ± 4)	198.1 (173.0 ± 5)
HOBr	−68.1 (−75.6 ± 9)	108.2 (84.0 ± 10)	153.1 (125.5 ± 10)	190.2 (164.0 ± 10)
HOI	−66.3 (−74.8 ± 8)	109.9 (85.0 ± 8)	154.8 (126.5 ± 8)	192.0 (165.0 ± 8)

[21] and nitrogen [6]. It will be interesting to test the reliability of the Marcus theory for S_N2 reactions at oxygen. The Marcus equation

$$\Delta H^{\neq}_{YX} = \Delta H^{\neq}_{0\,YX} + 0.5\Delta H + \left[\frac{(\Delta H)^2}{16\Delta H^{\neq}_{0\,YX}}\right] \quad (14)$$

relates the intrinsic barrier height of a non-identity substitution reaction to the corresponding intrinsic barrier height in the absence of a thermodynamic driving force and the central enthalpy difference between product and reactant ion–molecule complexes **3** and **1**. We can see that the barrier heights predicted by Marcus theory are within a few kJ/mol of the actual DFT computed values, the largest difference being only 3.4 kJ/mol. A plot of barriers calculated according to Eq. (14) vs. the corresponding hybrid DFT data gives a very good correlation (see Figs. 3 and 4, $R^2 = 0.995$).

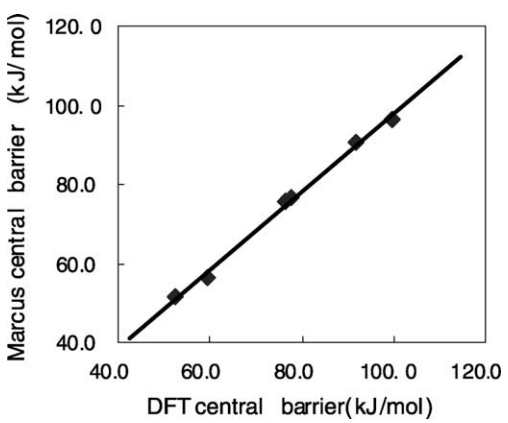

Fig. 3. Plot of central barrier from Eq. (14) vs. the same quantity obtained directly from the hybrid DFT method MPW1K/6-31+G(d,p).

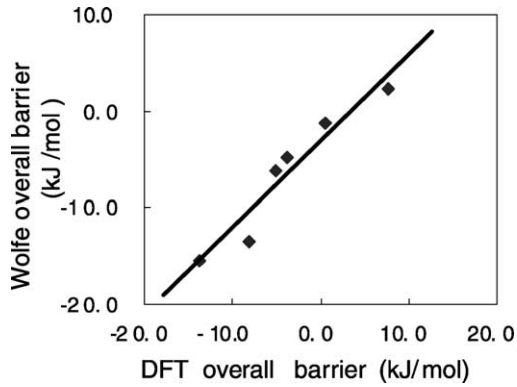

Fig. 4. Plot of overall barrier from Eq. (15) vs. the same quantity obtained directly from the hybrid DFT method MPW1K/6-31+G(d,p).

Since the property that is measured experimentally in a gas-phase S_N2 reaction is the overall barrier, rather than the central barrier, Wolfe et al. proposed the following modifications [24]:

$$\Delta H^{b}_{YX} = \Delta H^{b}_{0\,YX} + 0.5\Delta H^{ovr} + \left[\frac{(\Delta H^{ovr})^2}{16\Delta H^{\neq}_{0\,YX}}\right] \quad (15)$$

$$\Delta H^{b}_{0\,YX} = 0.5[\Delta H^{b}_{YY} + \Delta H^{b}_{XX}] \quad (16)$$

Eq. (15) facilitates predictions of experimentally more accessible quantities from data for the corresponding identity reactions. All of the values derived from Eq. (14) are lower than the corresponding calculated DFT results and the MSE is −2.7 kJ/mol. Although there is still a reasonable correlation between the overall barrier deduced from Eq. (15) with the overall barrier computed by the hybrid DFT method ($R^2 = 0.922$), the numerical results indicate that modification of the Marcus equation for estimating overall

barriers is less satisfactory than the original form for the central barriers.

4. Conclusions

Our investigation of the exchange reactions at saturated oxygen $Y^- + HOX \rightarrow HOY + X^-$ (Y, X = F, Cl, Br, I) at the MPW1K/6-31+G(d,p) level of theory leads to the following conclusions:

(1) For the identity S_N2 reactions $Y^- + HOY \rightarrow YOH + Y^-$ (Y = Cl, Br, I), the complexation energies (ΔH_{XX}^{comp}), central barrier heights ($\Delta H_{XX}^{\neq}$), and overall barriers (ΔH_{XX}^{b}) calculated by the MPW1K/6-31+G(d,p) method are very close to the corresponding G2(+) values. The MUEs for the $X^- + HOX$ (where X = Cl, Br, I) systems are only 1.23 kJ/mol (ΔH_{XX}^{comp}), 2.13 kJ/mol ($\Delta H_{XX}^{\neq}$), and 1.73 kJ/mol (ΔH_{XX}^{b}), respectively. The patterns of potential energy surfaces for the reactions $X^- + HOX \rightarrow XOH + X^-$ described by the MPW1K/6-31+G(d,p) level are analogous to the corresponding G2(+) results.

(2) The energy profile for the gas-phase non-identity S_N2 reactions at oxygen is described by an asymmetric double-well curve, with the following pathway for the reactions $Y^- + HOX$ ($Y \neq X$, Y, X = Cl, Br, I):

$$Y^- + HOX \rightarrow Y^- \cdots HOX \rightarrow [Y \cdots HO \cdots X]^{-\neq} \rightarrow YOH \cdots X^- \rightarrow HOY + X^-$$

As for the reactions $Y^- + HOF$ (Y = F, Cl, Br, I), the following reaction pathway is theoretically predicted:

$$Y^- + HOF \rightarrow Y^- \cdots HOF \rightarrow [Y \cdots HO \cdots F]^{-\neq} \rightarrow HF + OY^-$$

(3) The asymmetrical displacement reactions are exothermic only when the nucleophile is the heavier halide, unlike non-identity substitution reactions at carbon.

(4) For the reactions $Y^- + HOX$ (Y, X = Cl, Br, I), the forward central barrier heights $\Delta H_{YX}^{\neq}$ vary from 52.5 kJ/mol for the reaction $I^- + HOBr$ to 76.6 kJ/mol for the reaction $Br^- + HOCl$ and the reverse central barrier heights $\Delta H_{XY}^{\neq}$ vary from 77.6 kJ/mol for the reaction $Br^- + HOI$ to 99.7 kJ/mol for the reaction $Cl^- + HOI$. These $\Delta H_{YX}^{\neq}$ are lower than the intrinsic central barriers $\Delta H_{0\,YX}^{\neq}$ and the lowering is attributed to the effect of forward reaction exothermicity which ranges from −15.6 kJ/mol for $I^- + HOCl$ to −1.4 kJ/mol for $Br^- + HOCl$.

(5) All of the forward overall barriers ΔH_{YX}^{b} for the reactions $Y^- + HOX \rightarrow HOY + X^-$ are negative, which is similar to the identity reaction $X^- + HOX \rightarrow HOX + X^-$ and the non-identity exothermic reactions $Y^- + CH_3X$. The ΔH_{YX}^{b} values vary from −13.8 kJ/mol for $I^- + HOBr$ to −5.2 kJ/mol for $Br^- + HOCl$.

(6) The ion–molecule complexation energies at 0 K increase from 66.3 kJ/mol for $I^- \cdots HOBr$ to 207.0 kJ/mol for $F^- \cdots HOF$. These values are larger than those found for the corresponding carbon complexes. The $Y^- \cdots HOX$ complexation energies correlate well with the electronegativity of the halogen Y and the elongation parameter %O–H.

(7) The series of non-identity S_N2 reactions at oxygen obeys the Marcus equation. The central barriers estimated from the Marcus equation are very close to the directly calculated central barriers and a plot of the two data sets gives a good correlation ($R^2 = 0.995$). A modified equation used to estimate the overall barriers is found to be less reliable.

(8) The central barriers $\Delta H_{YX}^{\neq}$ and $\Delta H_{XY}^{\neq}$ exhibit a good linear correlation with the geometric looseness (%O–$X^{\neq}$ and %O–$Y^{\neq}$) of the transition state structures.

Acknowledgements

This work was supported by the Barbara and Kort Sino-Israel Post-Doctoral Fellowship Program and

the Israel Science Foundation, the Scientific Research Foundation for the Returned Chinese Scholars of State Education Ministry, and Scientific Research Foundation for the Young Teacher of Sichuan University.

References

[1] E. Erdik, M. Ay, Chem. Rev. 89 (1989) 1947, and references cited therein.
[2] R. Ulbrich, M. Famulok, F. Bosold, G. Boche, Tetrahedron Lett. 31 (1990) 1689.
[3] J.S. Helmick, K.A. Martin, J.L. Heinrich, M. Novak, J. Am. Chem. Soc. 113 (1991) 3459.
[4] T. Sherasky, L. Yusupova, Tetrahedron Lett. 36 (1995) 7701.
[5] R. Gareyev, S. Kato, V.M. Bierbaum, J. Am. Soc. Mass Spectrom. 12 (2001) 139.
[6] M. Bühl, H.F. Schaefer III, J. Am. Chem. Soc. 115 (1993) 9143.
[7] R.M. Minyaev, D.J. Wales, J. Phys. Chem. 98 (1994) 7942.
[8] M.N. Glukhovtsev, A. Pross, L. Radom, J. Am. Chem. Soc. 117 (1995) 9012.
[9] Y. Ren, H. Basch, S. Hoz, J. Org. Chem. 67 (2002) 2210.
[10] Y. Ren, J.L. Wolk, S. Hoz, Int. J. Mass Spectrom. 220 (2002) 1.
[11] B.J. Lynch, P.L. Fast, M. Harris, D.G. Truhlar, J. Phys. Chem. A 104 (2000) 4811.
[12] S. Parthiban, G. de Oliveira, J.M.L. Martin, J. Phys. Chem. A 105 (2001) 895.
[13] Y. Ren, J.L. Wolk, S. Hoz, Int. J. Mass Spectrom. 221 (2002) 59.
[14] R.A. Marcus, Annu. Rev. Phys. Chem. 15 (1964) 155.
[15] R.A. Marcus, J. Phys. Chem. 72 (1968) 891.
[16] W.J. Albery, Annu. Rev. Phys. Chem. 31 (1980) 227.
[17] M.J. Frisch, G.W. Trucks, H.B. Schlegel, G.E. Scuseria, M.A. Robb, J.R. Cheeseman, V.G. Zakrzewski, J.A. Montgomery, R.E. Stratmann Jr., J.C. Burant, S. Dapprich, J.M. Millam, A.D. Daniels, K.N. Kudin, M.C. Strain, O. Farkas, J. Tomasi, V. Barone, M. Cossi, R. Cammi, B. Mennucci, C. Pomelli, C. Adamo, S. Clifford, J. Ochterski, G.A. Petersson, P.Y. Ayala, Q. Cui, K. Morokuma, D.K. Malick, A.D. Rabuck, K. Raghavachari, J.B. Foresman, J. Cioslowski, J.V. Ortiz, B.B. Stefanov, G. Liu, A. Liashenko, P. Piskorz, I. Komaromi, R. Gomperts, R.L. Martin, D.J. Fox, T. Keith, M.A. Al-Laham, C.Y. Peng, A. Nanayakkara, C. Gonzalez, M. Challacombe, P.M.W. Gill, B. Johnson, W. Chen, M.W. Wong, J.L. Andres, C. Gonzalez, M. Head-Gordon, E.S. Replogle, J.A. Pople, GAUSSIAN 98, Revision A.7, Gaussian, Inc., Pittsburgh, PA, 1998.
[18] W.R. Wadt, P.J. Hay, J. Chem. Phys. 82 (1985) 284.
[19] B.J. Lynch, D.G. Truhlar, J. Phys. Chem. A 105 (2001) 2936.
[20] M.N. Glukhovtsev, A. Pross, L. Radom, J. Am. Chem. Soc. 118 (1996) 6273.
[21] M.N. Glukhovtsev, A. Pross, L. Radom, J. Phys. Chem. 100 (1996) 3498.
[22] B.A. Flowers, J.S. Francisco, J. Phys. Chem. A 105 (2001) 494.
[23] NIST Standard Reference Database Number 69, July 2001. Release (http://webbook.nist.gov/chemistry).
[24] S. Wolfe, D.J. Mitchell, H.B. Schlegel, J. Am. Chem. Soc. 103 (1981) 76942.